Zeitschrift: Helvetica Physica Acta
Band: 40 (1967)
Heft: 7

Artikel: Properties of several states in 41K near 8.9 MeV
Autor: Bloch, R. / Pixley, R.E. / Winkler, H.
DOI: https://doi.org/10.5169/seals-113796

Properties of Several States in ^{41}K near 8.9 MeV

by **R. Bloch, R. E. Pixley** and **H. Winkler**[1])
Physikinstitut der Universität Zürich

(11. V. 67)

Abstract. Resonance anomalies have been observed in protons elastically scattered from ^{40}A at three resonances near 1.1 MeV. Measurements at 90°, 125° and 141° indicate that the 1086, 1102 and 1108 keV resonances are formed by p-wave protons. The spin 1/2 assignment could be excluded on the basis of alpha-particle and gamma-ray angular distributions indicating that all three resonances are $J^{\pi} = 3/2^{-}$. A least squares fit was made to the elastic scattering data using the theoretical cross section folded with the measured resolution thereby determining Γ and Γ_p/Γ. The values of Γ, Γ_p/Γ and Γ_α are (7.9 ± 1.9) eV, (0.49 ± 0.16) and (0.032 ± 0.012) eV for the 1086 keV resonance; (21.9 ± 2.5) eV, (0.58 ± 0.08) and (0.064 ± 0.024) eV for the 1102 keV resonance and (5.1 ± 0.8) eV, (0.70 ± 0.15) and (0.019 ± 0.006) eV for the 1108 keV resonance.

Introduction

Many resonances are known [1–4] in ^{40}A(p, γ) ^{41}K. The level density is approximately one every 10 keV near 1.1 MeV, and the level widths are less than several keV. Gamma-ray yield measurements [5] indicate that some of the strongest gamma transitions are of the order of several eV. Spin assignments have been made for several of the strongest resonances on the basis of gamma-ray angular distributions [3, 6, 7]. Previous elastic scattering measurements [4, 8] failed to show resonance anomalies below 1.8 MeV. A recent good resolution measurement [9] of the elastic scattering cross section near 1.1 MeV and between 1.63 and 2.6 MeV, made concurrently with the present work, showed many narrow previously unreported resonances.

The present work was undertaken in order to measure the elastic scattering at several resonances near 1.1 MeV with a resolution and statistical accuracy sufficient to observe the anomalies, thereby determining the l-value of the protons forming the resonances. Additional measurements of gamma-ray and alpha-particle angular distributions permitted a unique spin assignment for these levels which when combined with the elastic scattering data, resulted in values of J^{π}, Γ and Γ_p/Γ. A preliminary report of some of this work has previously been given [10].

Experimental Method

The proton beam from the Van de Graaff accelerator was focused on a 0.5 mm entrance slit 50 cm in front of the 90°, $r = 50$ cm analyzing magnet. The focal proper-

[1]) Present address: California Institute of Technology, Pasadena, California.

ties of this magnet and the following 20° switching magnet were adjusted to give a second focus at the 1.5 mm wide stabilizing slits immediately before the target chamber. The switching magnet was 1 meter from the end of the 90° magnet and 2 meters from the target. The beam entered the differentially pumped target chamber, shown in Figure 1, through two canals in which the limiting aperture was 1.8 mm diameter. The region between the two canals was pumped by a 450 l/min, two stage mechanical pump and was maintained at a pressure at least 15 times lower than the pressure in the target chamber. The geometry of this system was designed to drop the pressure in front of the target as quickly and over as short a distance as possible in order to avoid straggling of the beam and the production of gamma rays outside the target area. Argon pressures up to 3 torr could be used in the target without overloading the pumping system. A 0.5 mg/cm^2 nickel foil limited the total target length to 10 mm and separated the chamber from the beam collector which was maintained at high vacuum. In order not to destroy the exit foil, it was necessary to run with some gas in the chamber for cooling and to limit the beam current to less than 1 μA. Four surface barrier detectors 4 mm in diameter were mounted in the chamber 6 cm from the target. Two detectors were located at 90° (one on each side of the beam) and one each at 125° and 141°. A 2 cm diameter brass cylinder with rectangular slits surrounded the target so that each counter saw approximately 4 mm of the 10 mm long target. A 7.6 × 7.6 cm NaI crystal for gamma-ray detection was located 2.5 cm above the center of the target chamber. Each detector was connected via preamplifier and amplifier to a single channel analyzer and scaler.

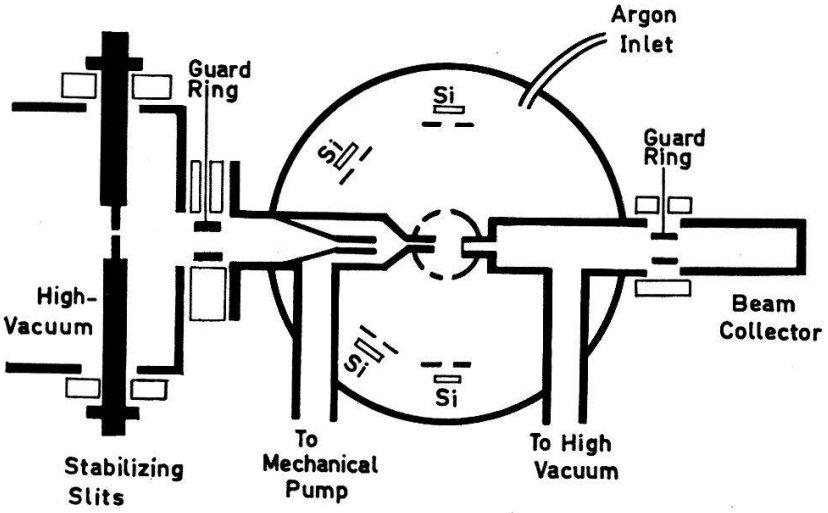

Figure 1

Scattering chamber and counter arrangement.

Considerable effort was devoted to obtaining good energy resolution. The current stabilized power supply of the 90° magnet was locked to a proton NMR signal. Slow as well as rapid field variations were less than an equivalent $\pm$ 10 eV at 1.1 MeV. An auxiliary stabilizer [11] for the Van de Graaff accelerator was used to improve the beam stability and resolution over that normally obtained with the corona stabilizer alone. The experimental resolution of the equipment was checked using the thin target excitation function of gamma rays near the 1102 keV resonance. Figure 2 shows the

gamma-ray yield as a function of energy measured with a 0.1 torr target pressure. The FWHM of this curve is 145 $\pm$ 10 eV. Although the resonance width of 22 eV (see following) and the target thickness of 35 eV are much less, the Doppler broadening due to the thermal motion of the target atoms is 87 eV FWHM at room temperature and thereby represents a sizeable fraction of the total resolution width. Assuming the various widths add quadratically, one finds the resolution of the incoming proton beam to be 108 eV FWHM.

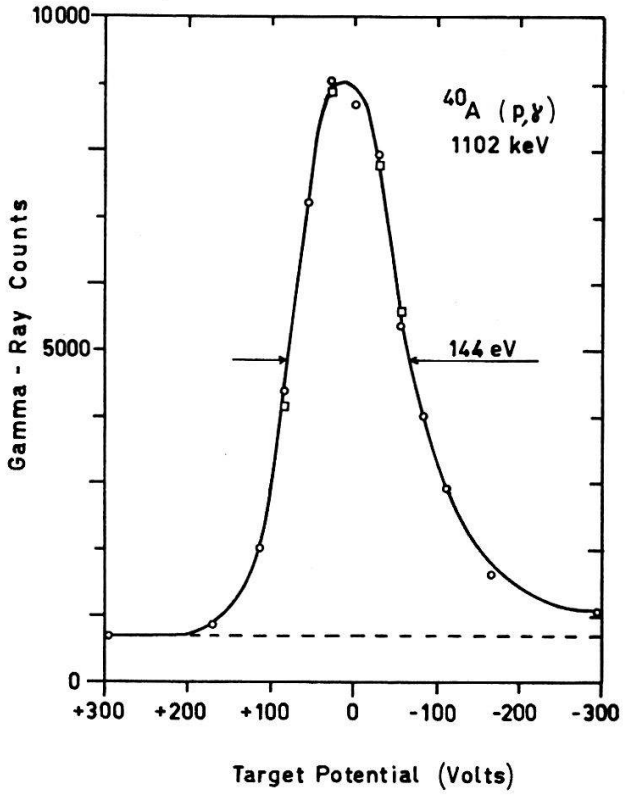

Figure 2

Gamma-ray yield at the 1102 keV resonance with a target pressure of 0.1 torr.

Slow variations in target pressure and beam integration were found troublesome during the several hour long measurements required to obtain a statistical accuracy in the proton scattering yield of better than 0.5%. Many rapid passes were therefore made in order to average out such variations. To facilitate rapid energy changes, the energy of the incoming protons was held constant while the target chamber potential was varied in 50 V steps between plus and minus 500 V. This system also insures good reproducibility of the 'local' energy scale while going over a resonance. The particle counter preamplifiers, the gas inlet system, the beam integrator and the first stage mechanical pump were all insulated from ground and connected to the target chamber potential. Since the beam stabilizer slits were located very close to the canal system of the target chamber, it was found necessary to introduce a guard ring connected to $-$ 1.2 kV between the two. A single pass over a resonance required approximately 30 minutes and consisted of 11 measurements of 110 μC each. Ten to 25 passes were made at each resonance with alternate ones in opposite directions.

The γ-ray counting rate was high enough (2×10^4 to 6×10^4 per 110 μC point at the resonance peaks) so that the γ-ray yield as a function of energy could be used to monitor the energy stability during the proton scattering measurements. Occasional energy shifts of up to 25 eV were noted. For a measurement point showing a shift greater than 15 eV, the data were discarded, the proton energy was corrected with the 90° magnet and the point remeasured.

The particle detectors had resolutions of less than 30 keV. Almost no background in the region near the elastic peak was observed with the argon pressure of 0.2 torr used for the scattering measurements. A wide channel was placed on the elastic peak extending down to 80% of the peak pulse height. The original detectors were somewhat unstable in the argon environment, and it was necessary to adjust the gain a few percent from time to time. Later counters with an epoxy edge protection were stable[2]).

Gamma-Ray Excitation Function and Elastic Scattering Data

Prior to the accurate elastic scattering measurements, a rough excitation curve for gamma rays and scattered protons was measured between 1075 and 1200 keV with 200 eV resolution. Many small resonances were observed in the gamma-ray yield, but only the three resonances at 1086, 1102 and 1108 keV showed scattering anomalies greater than the 3% counting statistics. A portion of the gamma-ray excitation curve is shown in Figure 3. Resonance energies and relative gamma-ray intensities are given in Table 1. The energy scale is based on the absolute energy measurement [5] of the resonance at 1101.8 $\pm$ 0.3 keV. Relative energies were reproducible to $\pm$ 0.1 keV. It is seen that many of the resonances previously reported are multiple in character.

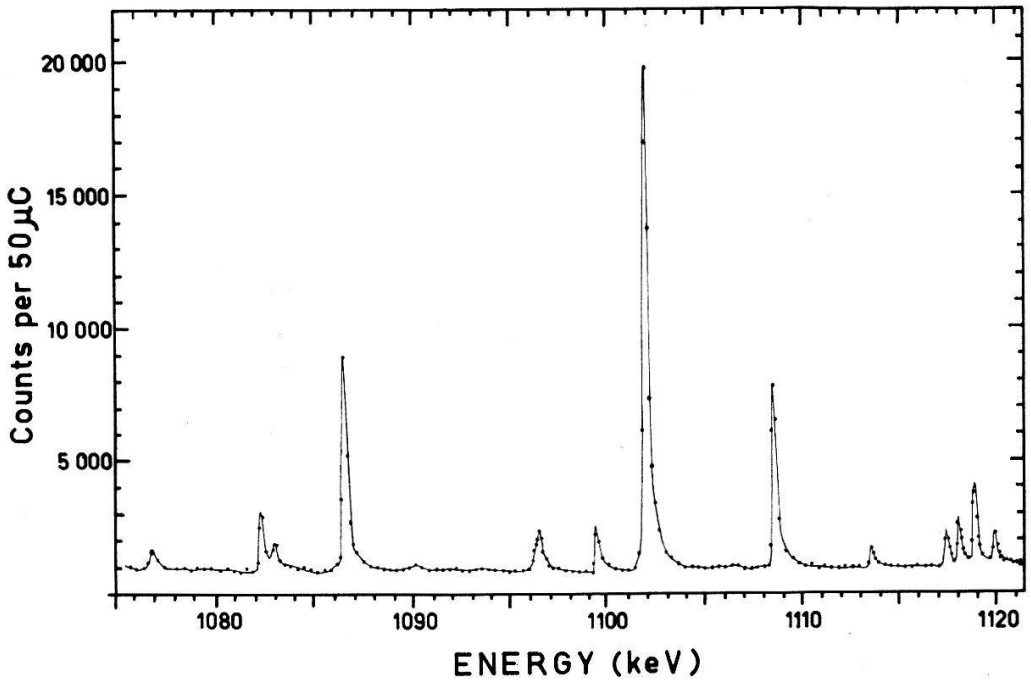

Figure 3

Gamma-ray excitation function.

[2]) We are indepted to Dr. J. BENN who prepared the original detectors and to Prof. V. MEYER who remade them with edge protection.

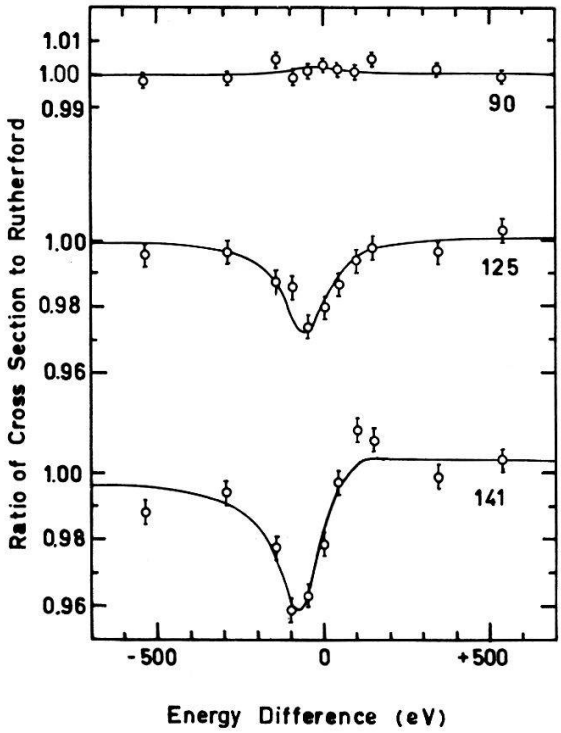

Figure 4

Elastic scattering data for the 1086 keV resonance. The solid curves are the best fit to the data for $J^{\pi} = 3/2^{-}$. Values of Γ and Γ_p/Γ are 7.9 ± 1.9 eV and 0.49 ± 0.16.

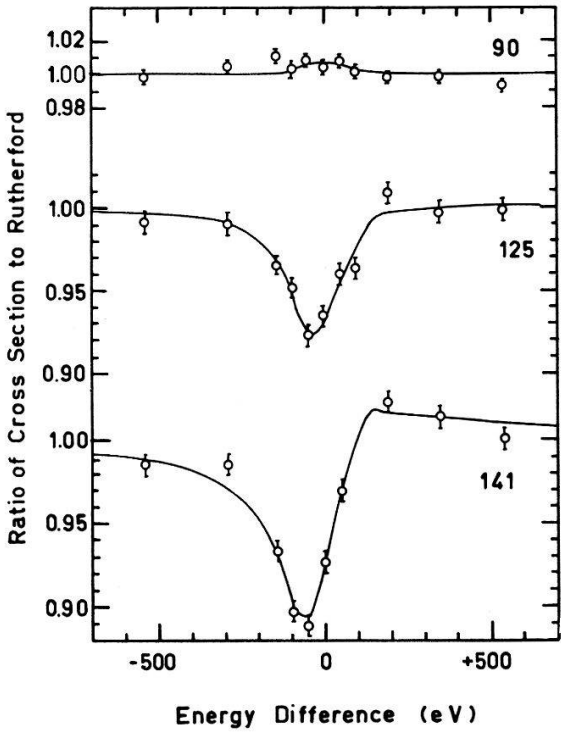

Figure 5

Elastic scattering data for the 1102 keV resonance. The solid curves are the best fit to the data for $J^{\pi} = 3/2^{-}$. Values of Γ and Γ_p/Γ are 21.9 ± 2.5 eV and 0.58 ± 0.08.

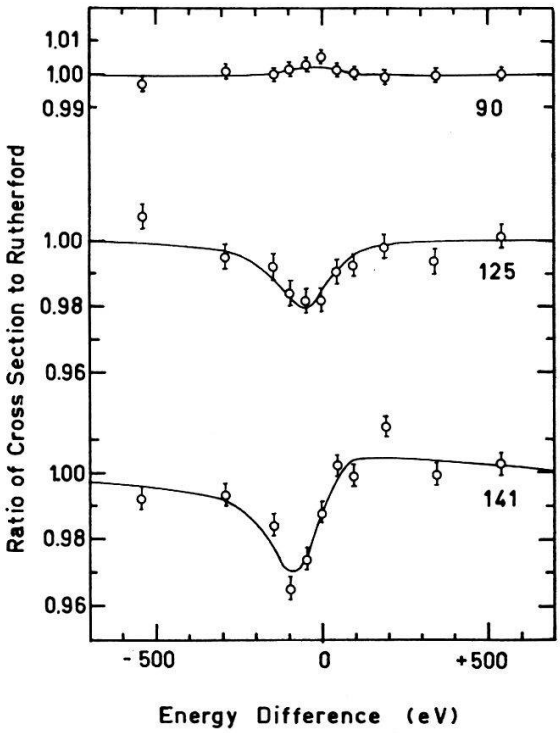

Figure 6

Elastic scattering data for the 1108 keV resonance. The solid curves are the best fit to the data for $J^{\pi} = 3/2^{-}$. Values of Γ and Γ_p/Γ are 5.1 ± 0.8 eV and 0.70 ± 0.15.

Table 1

Energies and gamma-ray intensities of resonances in ^{40}A(p, γ) relative to the resonance at 1101.8 ± 0.3 keV [5]

E_p (keV)	Relative γ-intensities	E_p (keV)	Relative γ-intensities	E_p (keV)	Relative γ-intensities
1076.65	0.03	1118.72	0.16	1162.76	0.10
1082.26	0.12	1119.82	0.07	1165.55	0.02
1082.90	0.05	1130.52	0.01	1168.88	0.07
1086.46	0.43	1137.09	0.02	1172.75	0.03
1096.19	(0.04)[a]	1138.74	0.03	1177.58	0.08
(1096.42)	(0.04)[a]	1140.03	0.09	1179.17	0.
1099.34	0.06	1141.86	0.08	1184.70	0.06
1101.80	1.00	1146.89	0.05	1186.31	0.07
1108.39	0.37	1150.28	0.04	1194.01	0.07
1113.45	0.04	1152.11	0.09	1195.70	0.05
1117.27	0.08	1154.02	0.10		
1117.92	0.10	1159.70	0.04		

[a] Probably an unresolved doublet as determined from the shape of the excitation function.

The normalized elastic scattering data for the multiple pass measurements at the 1086, 1102 and 1108 keV resonances are shown in Figures 4, 5 and 6. The counting rates at each energy were multiplied by E^{+2} in order to take out the energy dependence of the Rutherford scattering cross section. The solid curves are the least squares fit to the data at each resonance of the theoretical cross section [12] folded with the experimental energy resolution as determined from the gamma-ray yield. For the present case in which potential scattering (other than Coulomb) is completely negligible, only J^π and the two parameters, Γ and Γ_p/Γ, occur in the formula for elastic scattering at a narrow resonance. Since the absolute value of the elastic scattering cross section cannot be measured with sufficient accuracy, we have included three additional parameters in the least squares fit of each resonance representing the normalizing factors for the experimental data at each angle (a brief description of the least squares method is given in the appendix). It is clear from the general character of the data, namely a small peak at 90° and a large dip at both 125° and 141°, that only $J^\pi = (1/2)^-$ and $(3/2)^-$ corresponding to p-wave protons need be considered.

Table 2

Values of Γ and Γ_p/Γ for $J^\pi = 1/2^-$ and $3/2^-$ giving the best fits to the elastic scattering data of the 1086, 1102 and 1108 keV resonances. Also listed are the values of the total χ^2 and the partial values at each angle.

E_0 (keV)	J^π	Γ (eV)	Γ_p/Γ	$\chi^2_{90°}$	$\chi^2_{125°}$	$\chi^2_{141°}$	χ^2
1086	$3/2^-$	7.9 ± 1.9	0.49 ± 0.16	15.6	9.1	22.7	47.4
	$1/2^-$	15.0 ± 4.9	0.51 ± 0.18	17.7	7.3	25.2	50.3
1102	$3/2^-$	21.9 ± 2.5	0.58 ± 0.08	15.3	10.8	12.0	38.3
	$1/2^-$	40.9 ± 6.2	0.63 ± 0.10	16.7	11.2	16.7	44.7
1108	$3/2^-$	5.1 ± 0.8	0.70 ± 0.15	8.0	11.4	20.6	40.1
	$1/2^-$	8.8 ± 1.5	0.79 ± 0.16	5.3	11.3	21.2	37.8

In Table 2 are listed the values of Γ, Γ_p/Γ, their errors, the total minimum χ^2 and the partial χ^2 at each angle. It is seen that the accuracy of the measurements is not sufficient to make a meaningful choice between $(1/2)^-$ and $(3/2)^-$ for the 1086 and 1108 keV resonances. The values of χ^2 lie between 37 and 53 which is to be compared with the expected value of 28 corresponding to the 33 measured points at each resonance less 5 adjustable parameters. The rather high values of χ^2 are not too unreasonable since the error of each measured point is known to be somewhat larger than the counting statistical error used in the calculation and since some approximations were used in connection with the resolution function. The uncertainty of Γ and Γ_p/Γ given in Table 2 were obtained using the actual value of χ^2 listed in the table. It is noteworthy that no energy shift parameter is necessary as the energy position of the computed elastic scattering curves is completely determined by the measured gamma-ray curve (see Appendix).

Alpha-Particle Measurements

The choice between $J^\pi = 1/2^-$ and $3/2^-$ can in principle be made on the basis of the angular distribution of alpha particles leading to the $3/2^+$ ground state of ^{37}Cl. The distribution is isotropic for a $J = 1/2$ state in ^{41}K and of the form $1 + a_2 P_2(\cos\theta)$

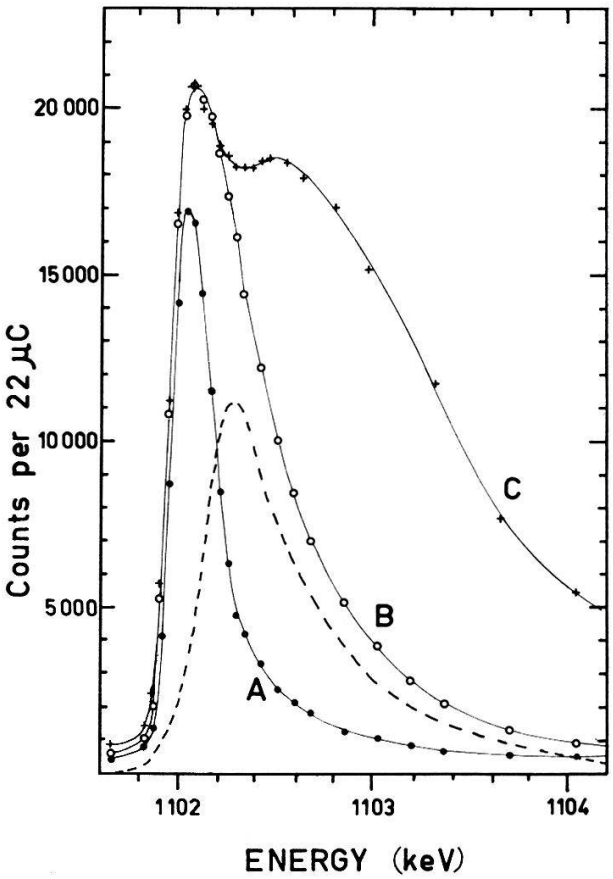

Figure 7

Gamma-ray yields at the 1102 keV resonance with various target pressures. Curve A is with a pressure of 0.63 torr, curve B is with 1.47 torr and curve C is with 3.0 torr. The difference between curves B and A is equivalent to the alpha-particle yield as seen by the particle detectors with a target pressure of 2.1 torr (dashed curve).

for a $3/2^-$ state. From a $3/2^-$ state in ^{41}K, both p-wave and f-wave alpha particle emission to the ground state of ^{37}Cl are possible. Since the penetration factors differ by only a factor of 7, f-wave emission can compete with p-wave emission making it necessary to consider a_2 as a parameter depending on the mixing ratio. The value of a_2 can lie between -1 and $+4/5$ and is in fact zero for two particular values of the mixing ratio. Thus, an angular distribution found to be isotropic can not unambigu ously be assigned $J = 1/2$ without further experimental confirmation.

Alpha particle yields were measured at the peak of each resonance with a target pressure of 2 torr. Even with this pressure, the alpha counting rates were only of the order of 1 per minute. Although the alpha particles have an energy of 2.6 MeV compared with 1.1 MeV for the scattered protons, the spectrum of pile-up protons extends to 2.2 MeV making channel placement difficult. For this reason it was convenient to store simultaneously the spectra of the 90°, 125° and 141° detectors using pulse routing techniques and to choose the proper energy channel after the measurement. Each spectrum showed a region between the alpha peak and the end of the pile-up spectrum which was free of background pulses. Measurements off resonance showed no alpha counts.

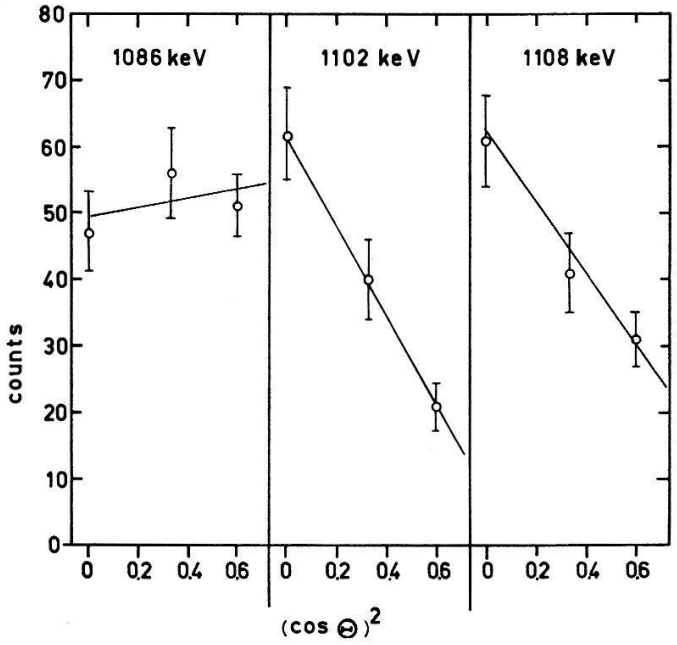

Figure 8

Alpha particle angular distributions for the 1086, 1102 and 1108 keV resonances. The solid curves represent the best two parameter fit to the data at each resonance.

Due to the low alpha counting rates it was not feasible to measure the excitation function for alpha emission very accurately. The target thickness and energy resolution were therefore obtained from gamma-ray measurements using various target pressures. Figure 7 shows the gamma-ray yield for target pressures corresponding to a) the 3 mm section of target in front of the region seen by the detectors, b) the 7 mm length of target including the region seen by the detectors and c) a semi-thick target showing the LEWIS effect peak [13]. The difference between curves b) and a) corre-

sponds to the alpha particle excitation function for the 2.0 torr target pressure used in the alpha particle measurements. One sees that the peak of the alpha particle curve is 50% of the thick target yield at the Lewis peak. From proton measurements, it was found that the section of the target seen by the three particle detectors was within 10% of being the same. The alpha particle counting were corrected for differences in target length and detector solid angles using the proportionality determined from the proton rates off resonance which have been shown to be very nearly Rutherford scattering cross section.

The alpha particle angular distributions are shown in Figure 8. It is clear that the distributions for the 1102 and 1108 keV resonances are strongly anisotropic and therefore consistent with only $J^\pi = 3/2^-$ while that of the 1086 keV resonance is very nearly isotropic. The solid curves represent the best two parameter fit to the data of the form $K\ (1 + A\ \cos^2\vartheta)$. The values determined for A are 0.14 ± 0.09, -1.10 ± 0.15 and -0.87 ± 0.22 for the 1086, 1102 and 1108 keV resonances respectively. The quoted uncertainties are derived from the expected χ^2 which in these three cases was slightly larger than the actual χ^2. Although the value of A for the 1086 keV resonance determined from the best fit using two parameters does not include $A = 0$, a one parameter fit assuming $A = 0$ is consistent with the data thus allowing an assignment of either $1/2^-$ or $3/2^-$.

The alpha particle partial widths have been determined from the absolute value of the measured alpha particle yield. Using the values of Γ_p/Γ determined from the elastic scattering one finds Γ_α to be either 0.032 ± 0.012 eV or 0.064 ± 0.024 eV for the 1086 keV resonance depending upon whether the spin is 3/2 or 1/2, 0.040 ± 0.010 eV for the 1102 keV resonance and 0.019 ± 0.006 eV for the 1108 keV resonance.

Gamma-Ray Angular Distribution Measurements

Although the scattering chamber was not designed for gamma-ray angular distribution work, it was possible to measure at 0° and 90° with only small absorption corrections by removing the beam collector and one of the 90° particle detectors. For these measurements, the beam current was monitored on a Ta beam stopper 10 mm in back of the entrance canal. A $7{,}6 \times 7.6$ cm NaI crystal 2.5 cm above the target was used as monitor and a second 7.6×7.6 cm crystal was positioned 23 cm from the target at either 0 or 90°. The spectra of both detectors were stored simultaneously in the multichannel analyzer. Pulse height stability was checked with the 4.43 MeV gamma rays from a Po-Be source before and after each 20 minute measurement. A target pressure of 1.4 torr was used corresponding to curve B of Figure 7 and the proton energy was adjusted for peak gamma-ray yield.

The 0° to 90° gamma-ray intensity ratio of the 8.9 MeV ground-state transition was measured for the 1086 and 1108 keV resonances. The 0° to 90° ratio was found to be 1.60 ± 0.20 for both resonances. The accuracy is sufficient to exclude the $J = 1/2$ assignment which would have resulted in an isotropic distribution. The data are in fact consistent with a $3/2 - 3/2$, pure dipole transition which results in a 0° to 90° ratio of 1.75. Thus, on the basis of the gamma-ray measurements in conjunction with the elastic scattering work, the 1086 and 1108 keV resonances are found to be $J^\pi = 3/2^-$.

Discussion

Previous measurements of gamma-ray angular distributions have assigned spins of 5/2 to the 1086 keV resonance [3], 3/2 or 5/2 to the 1102 keV resonance [3, 7] and 3/2 to the 1108 keV resonance [6]. The present work is in agreement with the assignments for the 1102 and 1108 keV resonances and removes the 3/2–5/2 ambiguity for the former. The spin assignment as well as the 0° to 90° gamma-ray intensity ratio of 0.50 ± 0.05 determined in Reference [3] for the 1086 keV resonance is not confirmed by the present measurements for which the 0° to 90° ratio was found to be 1.60 ± 0.20. No explanation for this large discrepancy is apparent. Odd parity for the 1108 keV resonance as suggested in Reference [6] on the basis of a large dipole to quadrupole mixing ratio is verified by the present elastic scattering measurement.

The elastic scattering measurements of KEYWORTH et al. [9] are consistent with the present work for the 1086 and 1102 keV resonances. No mention was made by them of the 1108 keV resonance which was apparently overlooked in their measurements. Their data which were obtained at a single scattering angle, determined the angular momentum of the resonance protons but gave no information regarding the 3/2, 1/2 spin choice and the value of Γ_p/Γ and Γ.

The $l = 3$ to $l = 1$ mixing ratios for alpha emission as determined from the measured alpha particle angular distributions are given in Table 3. The distribution function calculated from the tables of SHARP et al. [14] is

$$W(\vartheta) = 1 + (1 + x^2)^{-1} \left(-\frac{4}{5} + \frac{6}{5}\, x \cos\delta + \frac{4}{5}\, x^2 \right) P_2 (\cos\vartheta)$$

where x is the amplitude mixing ratio of f to p-wave alphas and δ is the difference in coulomb phases for p and f-wave alphas which is 137°. It is seen that the alpha decay of the 1102 and 1108 keV resonances is primarily p-wave while that of the 1086 keV resonance is mixed with both of the possible values of the mixing ration containing an appreciable f-wave component.

Also listed in Table 3 are the dimensionless reduced widths θ^2 for proton and alpha particle emission. The normalization employed is

$$\Theta_x^2 = \frac{\Gamma_x A_l \mu R}{3 \hbar^2 k}$$

Table 3

Values of x, the amplitude ratio of f to p-wave alpha emission and θ^2, the dimensionless proton and alpha particle reduced widths

E_0 (keV)	x	$\theta^2_{\alpha, l=1}$	$\theta^2_{\alpha, l=3}$	θ^2_p
1086	$+0.7 \pm 0.1$	8×10^{-4}	3×10^{-3}	2.1×10^{-3}
	or			
	-1.9 ± 0.15	3×10^{-4}	7×10^{-3}	
1102	-0.3 ± 0.3	1.4×10^{-3}	10^{-4}	7.0×10^{-3}
1108	$+0.05 \pm 0.15$	7×10^{-4}	0	2.0×10^{-3}
	or			
	-0.7 ± 0.2	5×10^{-4}	2×10^{-3}	

where Γ_x is the particle width, R is the interaction radius taken as 1.3 $(M_1^{1/3} + M_2^{1/3}) \times 10^{-13}$ cm, A_l^{-2} is the penetration factor evaluated [15] at the interaction radius, μ is the reduced mass of the reaction products and k is the wave number of relative motion. The reduced widths are very sensitive to the choice of the interaction radius. A 5% change in R affects a factor of 1.8 change in Θ_α^2 and a factor of 1.4 in Θ_p^2. It is seen that Θ_p^2 lies between (2 and 7) $\times 10^{-3}$ while the dimensionless reduced widths for $l = 1$ alpha emission are an order of magnitude smaller.

It is perhaps significant that the three strongest resonances in ^{40}A(p, γ) below 1.4 MeV have $J^\pi = 3/2^-$ and lie at roughly the expected energy in ^{41}K corresponding to the isobaric analogue of the second excited state in ^{41}A. It is known [16] from the d, p reaction on ^{40}A that the second excited state of ^{41}A is formed by $l_n = 1$ stripping and is thereby either $J^\pi = 1/2^-$ or $3/2^-$. The analogue of the fourth and sixth excited states in ^{41}K are reported [10] at proton energies of 1.87 and 2.45 MeV. Using this information along with the proton widths and the level spacings in ^{41}A corrected for neutron-proton level shifts [16], one would expect the analogue of the second excited state in ^{41}A to lie at a proton energy of 1.1 to 1.2 MeV. The present work therefore strongly suggests that the 1086, 1102 and 1108 keV resonances represent, at least in part, the isobaric analogue of the second excited state in ^{41}A and that the second excited state in ^{41}A is $J^\pi = 3/2^-$.

Acknowledgements

This work has been supported in part by the Swiss National Foundation. The authors wish to thank Prof. V. Meyer and Prof. H. Staub for helpful suggestions. The private communication from Dr. G. A. Keyworth regarding the Duke measurements prior to publication is greatfully acknowledged.

Appendix

The differential elastic scattering cross section near an isolated resonance relative to the non-resonant potential scattering cross section can be written in the form [12]

$$\frac{\sigma}{\sigma_{pot}}(\vartheta, E) = 1 + \frac{(E - E_0)\, A(\vartheta) + B(\vartheta)}{(E - E_0)^2 + \Gamma^2/4} \tag{1}$$

where E is the particle energy, E_0 is the resonance energy and $A(\vartheta)$ and $B(\vartheta)$ are angle factors which depend upon J^π, Γ, Γ_p/Γ. At the 1.1 MeV proton energy of the present work, the nonresonant potential scattering from ^{40}A is, to a high degree of accuracy, the point charge Coulomb scattering cross section. For this case the angle factors are given by

$$A(\vartheta) = u\, \Gamma \cos\beta$$

$$B(\vartheta) = \frac{\Gamma^2}{4}(u^2 + 2\, u \sin\beta + v^2) \tag{2}$$

where

$$u = \frac{2J+1}{\gamma}\frac{\Gamma_p}{\Gamma}\left(\sin\frac{\vartheta}{2}\right)^2 P_l(\cos\vartheta)$$

$$v = \frac{2}{\gamma}\frac{\Gamma_p}{\Gamma}\left(\sin\frac{\vartheta}{2}\right)^2 P_l^1(\cos\vartheta)$$

$$\beta = 2\left[\gamma \ln\left(\sin\frac{\vartheta}{2}\right) + \sum_0^l \arctan\frac{\gamma}{l'} - \frac{\pi}{2}\right]$$

$$\gamma = Z_1 Z_2 e^2 \hbar^{-1} [M_1(2E)^{-1}]^{1/2}.$$

A measurement of the undistorted resonance anomaly is possible only if the experimental resolution is considerably narrower than Γ. When this is not the case, as in the present work, the energy dependence of the normalized yield of elastically scattered protons at a specified angle is obtained by folding the theoretical cross section with the experimental resolution. This leads to

$$Y(E,\vartheta) = 1 + \int G(E'-E)\frac{\sigma}{\sigma_{pot}}(\vartheta, E')\,dE' \tag{3A}$$

where $G(E'-E)$ is the normalized resolution function including the effects of energy spread of the incoming beam, target thickness and Doppler broadening. The integration is taken over the energy range for which G is non-zero. In the present work, the FWHM of the resolution function was 7 to 23 times the resonance width and could therefore be approximated with good accuracy by the measured gamma-ray excitation function. Making use of this approximation for the resolution function along with a change of integration variable, one can write Equation (3A) as

$$Y(E,\vartheta) = 1 + \left[\int N_j(E')\,dE'\right]^{-1}\int N_j(E'')\left[\frac{(E-E'')A+B}{(E-E'')^2+\Gamma^2/4}\right]dE''. \tag{3B}$$

It is seen that the resonance energy E_0 does not appear explicitly in the expression (3B). In order to perform the integrations of Equation (3B), parabolas were passed through each set of three points of the gamma-ray excitation function and the integration carried out analytically over each section of the curve. The gamma-ray counting rate was large enough so that statistical uncertainties in $N(E)$ could be neglected.

A least squares fit was made between the measured data $N(\vartheta_i, E_j)$ compensated for the very slight E^{-2} variation of the non-resonant yield and the function $Y(E,\vartheta)$. The sum of the weighted quadratic deviations

$$\chi^2 = \sum_{ij}[N(\vartheta_i, E_j) - k_i\,Y(\vartheta_i, E_j)]^2\,N^{-1}(\vartheta_i, E_j) \tag{4}$$

contains the parameters Γ and Γ_p/Γ as well as normalizing factors k_i at each angle of observation ϑ_i. In the present work this amounts to a 5 parameter fit. A Taylor series expansion for χ^2 is made about trial values of the five parameters. The elements $m_{\mu\nu}$ of the 5×5 coefficient matrix M for the normal equation are

$$m_{\nu\mu} = \sum_{ij}\frac{\partial F_{ij}}{\partial P_\nu}\frac{\partial F_{ij}}{\partial P_\mu}N^{-1}(\vartheta_i, E_j) \tag{5}$$

where F_{ij} is equal to k_i. $Y(\vartheta_i, E_j)$ and P_ν and P_μ are any two of the five parameters. The partial derivatives are evaluated at the trial values of the parameters and the differentiation with respect to Γ and Γ_p/Γ is performed inside the integral (see Equation (3B)). The solution to the system of equations yields corrections to the trial values of the parameters. Better trial values are then obtained by iteration. The uncertainty σ_ν of the parameter P_ν is

$$\sigma_\nu = [m_{\nu\nu}^{-1}\, \chi^2\, f^{-1}]^{1/2} \tag{6}$$

where $m_{\nu\nu}^{-1}$ is a diagonal element of the inverted M matrix and f is the number of degrees of freedom. The expected value of χ^2 is f. In the present work, there were 33 measured points and five parameters resulting in 28 degrees of freedom.

References

[1] K. J. Broström, T. Huus and J. Koch, Nature *162*, 695 (1948).
[2] S. E. Arnell, Nucl. Phys. *24*, 500 (1961).
[3] I. Kohno, J. Phys. Soc. Japan *18*, 1709 (1963).
[4] J. Cohen-Ganouna, M. Lambert and J. Schmouker, Nucl. Phys. *40*, 82 (1963).
[5] R. Bloch, R. E. Pixley, H. Staub, F. Waldner, H. Winkler, Helv. phys. Acta *37*, 722 (1964).
[6] S. E. Arnell and P. O. Persson, Arkiv Fysik *27*, 41 (1964).
[7] A. K. Valter, Yu. P. Antufev, E. G. Kopanets, A. N. Lvov and S. P. Tsytko, Translated in Academy of Sciences of the USSR, N. Y. Bulletin, Physics series *26*, 423 (1964).
[8] A. C. L. Barnard and C. C. Kim, Nucl. Phys. *28*, 428 (1961).
[9] G. A. Keyworth, G. C. Kyker jr., E. G. Bilpuch and H. W. Newson, Phys. Letters *20*, 281 (1966) and private communication G. A. Keyworth.
[10] H. Winkler, R. E. Pixley and R. Bloch, Bull. Am. phys. Soc. [11], *10*, 1204 (1965).
[11] R. E. Pixley and R. Bloch, Helv. phys. Acta *39*, 209 (1966).
[12] J. M. Blatt and L. C. Biedenharn, Rev. mod. Phys. *24*, 258 (1952).
[13] H. W. Lewis, Phys. Rev. *125*, 937 (1962).
[14] W. T. Sharp, J. M. Kennedy, B. J. Sears and M. G. Hoyle (Unpublished Atomic Energy of Canada Ltd. Report CRT 556 (1954).
[15] A. V. Luk'yanov, I. V. Teplov and M. K. Akimova, *Tables of Coulomb Wave Functions* (Translation), Pergamon Press Ltd., London (1965).
[16] E. Kashy, A. M. Hoogenboom and W. W. Buechner, Phys. Rev. *124*, 1917 (1961).
[17] R. G. Thomas, Phys. Rev. *88*, 1109 (1952).